Geochemistry Geophysics Geosystems G3
AN ELECTRONIC JOURNAL OF THE EARTH SCIENCES
Published by AGU and the Geochemical Society

Article
Volume 5, Number 8
24 August 2004
Q08D10, doi:10.1029/2003GC000668
ISSN: 1525-2027

Crystallinity of foraminifera shells: A proxy to reconstruct past bottom water $CO_3^{=}$ changes?

Franck C. Bassinot
LSCE-IPSL, Unité Mixte CEA-CNRS, Domaine du CNRS, Gif sur Yvette, 91190, France (franck.bassinot@lsce.cnrs-gif.fr)

Also at Department of Earth Sciences, University of Cambridge, Cambridge, UK

Frédéric Mélières
Laboratoire de Géologie, MNHN, 75005 Paris, France

Marion Gehlen and Camille Levi
LSCE-IPSL, Unité Mixte CEA-CNRS, Domaine du CNRS, Gif sur Yvette, 91190, France

Laurent Labeyrie
LSCE-IPSL, Unité Mixte CEA-CNRS, Domaine du CNRS, Gif sur Yvette, 91190, France

Also at Département de Physique, Université Versailles-St Quentin, Versailles, France

[1] The reconstruction of past changes in bottom water $CO_3^{=}$ is central to evaluating competing oceanic scenarios that deal with long-term variations in atmospheric pCO_2. In search of a quantitative bottom water $CO_3^{=}$ proxy, we analyzed the variations of calcite crystallinity of planktonic foraminifera *Globigerinoides ruber* shells picked from core top samples along three depth transects: Ontong Java Plateau and the northeast margin of Irian Jaya, in the western equatorial Pacific, and the Sierra Leone Rise, in the eastern tropical Atlantic. The strong empirical relationship between calcite crystallinity (inferred from the full width at half maximum (FWHM) of calcite (104) X-ray diffraction peak) and bottom water saturation relative to calcite (ΔCO_3) shows that foraminifera calcite crystallinity could be a promising proxy for the reconstruction of upper Pleistocene bottom water carbonate ion concentration.

Components: 6906 words, 5 figures, 2 tables.

Keywords: bottom water CO_3; calcite crystallinity; carbonate dissolution; foraminifers.

Index Terms: 4267 Oceanography: General: Paleoceanography; 3954 Mineral Physics: X ray, neutron, and electron spectroscopy and diffraction.

Received 25 November 2003; **Revised** 23 April 2004; **Accepted** 23 June 2004; **Published** 24 August 2004.

Bassinot, F. C., F. Mélières, M. Gehlen, C. Levi, and L. Labeyrie (2004), Crystallinity of foraminifera shells: A proxy to reconstruct past bottom water $CO_3^{=}$ changes?, *Geochem. Geophys. Geosyst.*, *5*, Q08D10, doi:10.1029/2003GC000668.

Theme: Biogenic Calcium Carbonate **Guest Editor:** Peggy Delaney

1. Introduction

[2] On glacial to interglacial timescale, carbonate compensation is believed to maintain the global ocean alkalinity budget at steady state. Because ocean water alkalinity feeds back on atmospheric pCO_2, *Broecker and Peng* [1987] showed that $CaCO_3$ preservation on the seafloor may play a significant role in the oceanic scenarios that deal with glacial-interglacial changes in atmospheric pCO_2 [e.g., *Boyle*, 1988; *Broecker and Peng*, 1989; *Archer and Maier-Reimer*, 1994]. The mechanisms by which the alkalinity balance is achieved vary from one scenario to another. Thus some of those scenarios might be tested through their implications in terms of glacial-interglacial changes in the water column carbonate ion concentration and/or the amplitude of deep-sea carbonate dissolution. As a result, the quantitative reconstruction of both the vertical and geographical distributions of seawater carbonate chemistry (pH, $CO_3^{=}$) since the Last Glacial Maximum has been the focus of many recent studies [*Sanyal et al.*, 1995; *Broecker and Clark*, 2001a; *Anderson and Archer*, 2002]. These studies yielded quite contrasting conclusions (see, for instance, the difference in pH reconstruction by *Sanyal et al.* [1995] and *Anderson and Archer* [2002]). We are still in demand, therefore, for a reliable proxy of bottom water carbonate ion concentrations.

[3] *Lohmann* [1995] made the case that the weight of foraminifera shells picked from a narrow size range provides a measure of the extent of dissolution and in so doing has the potential to serve as a paleocarbonate ion proxy. This index was evaluated by *Broecker and Clark* [2001b] and used to analyze deep-sea carbonate ion at the LGM [*Broecker and Clark*, 2001a]. However, recent data [*Barker and Elderfield*, 2002] indicate that the weight of foraminifera shells may be largely dependent upon conditions that prevailed at the sea surface during formation of the shells, such as the surface water $CO_3^{=}$. This dependency upon surface water conditions is expected to translate into biases when using the proxy to reconstruct deep-sea carbonate ion changes at the LGM [*Bijma et al.*, 2002].

[4] In this paper, we evaluate the potential of calcite crystallinity measured from planktonic foraminifera shells deposited on the seafloor as a quantitative proxy for reconstructing changes in bottom water $CO_3^{=}$. Following the approach by *Barthelemy-Bonneau* [1978] and *Bonneau et al.* [1980], we analyzed the down slope evolution of calcite crystallinity of planktonic foraminifera shells obtained from core top samples along three bathymetric depth transects: Ontong Java Plateau and the northeast margin of Irian Jaya, in the western equatorial Pacific, and the Sierra Leone Rise, in the eastern tropical Atlantic.

2. Calcite Crystallinity of Planktonic Foraminifera Shells

[5] The crystallinity, measured by X-Ray Diffraction (XRD), is related to the degree of perfection of a given crystal lattice [e.g., *Lipson and Steeple*, 1970]. Following the work by *Mélières* [1978], we used the full width at half maximum (FWHM) of the (104) calcite X-ray diffraction peak (given in $^{\circ}2\theta$) as an indication of the degree of crystallinity of foraminifera shells. Shells showing a narrow (104) calcite peak on XRD powder diagrams are interpreted as being better crystallized than those showing a broader diffraction peak. Ultimately, XRD peak broadening depends on two main parameters at the lattice level: (1) it can be related to strain within the crystal structure, or (2) it can reflect the granulometry of the perfectly crystallized subdomains (hereafter referred to as ''crystallites'') that constitute the whole crystal. In the later case, peak broadening results from the slight misalignment of crystallites with respect to each other (''mosaic'' structure of the crystal lattice); the smaller the average size of these crystallites, the broader the diffraction peaks [e.g., *Lipson and Steeple*, 1970].

[6] Although a complete discussion of what causes peak broadening in foraminiferal calcite exceeds the goal of this paper, our data together with SEM observations of foraminifera biomineralization processes indicate that peak broadening is likely driven by changes in crystallite size.

[7] *Bonneau et al.* [1980] studied five planktonic foraminifera species picked from surface sediments sampled along a depth transect on Ontong Java Plateau. They showed that the calcite crystallinity of foraminifera tests improves (thinning of calcite (104) diffraction peak) as dissolution increases along the depth transect (Figure 1), which indicates that poorly crystallized calcite is removed preferentially as dissolution proceeds. As seen in Figure 1, it is also striking that the inter-species offsets in calcite (104) FWHM are coherent with the dissolution sensitivity ranking of planktonic foraminifera [e.g., *Berger*, 1968, 1970]. *Globoro-*

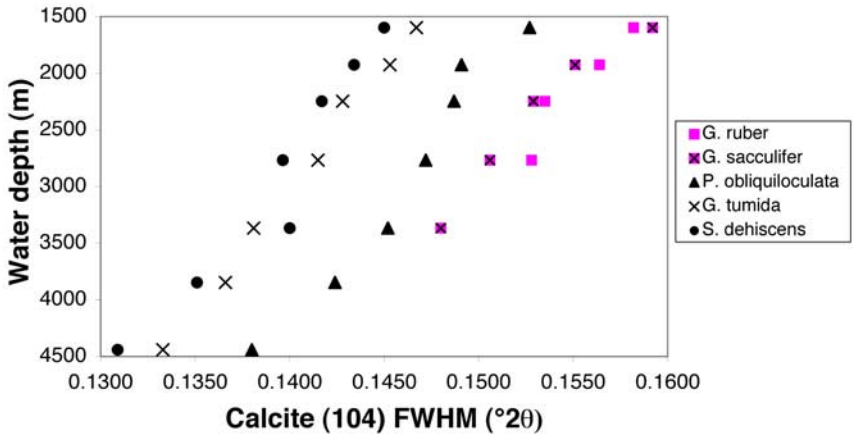

Figure 1. Profiles of water depth versus calcite (104) full width at half maximum (FWHM) of five planktonic foraminifera species picked from surface samples, Ontong Java Plateau, western equatorial Pacific (data from *Bonneau et al.* [1980]).

talia tumida and *Sphaeroidinella dehiscens*, which are two species among the most dissolution-resistant, show the thinnest calcite (104) peak (well crystallized), whereas *Globigerinoides ruber and Globigerinoides sacculifer*, which are known to be very sensitive to dissolution, show the broadest calcite (104) peak (poorly crystallized). *Pulleniatina obliquiloculata* has an intermediate calcite (104) FWHM, in good accordance with its intermediate ranking in dissolution sensitivity compared to the four other species described above (Figure 1). These results suggest that calcite crystallinity is probably of key importance in setting the resistance to dissolution of planktonic foraminifera tests. The link between foraminiferal calcite crystallinity and its dissolution susceptibility appears to be particularly promising in search for a quantitative dissolution index that could be tied to carbonate ion changes in the deep sea.

[8] In order to evaluate the potential of foraminiferal calcite crystallinity as a $CO_3^{=}$ proxy, we completed the study from *Bonneau et al.* [1980] by analyzing the relationship between *Globigerinoides ruber* crystallinity and bottom water saturation relative to calcite ($\Delta CO_3^{=}$) along two additional depth transects located in the tropical western Pacific Ocean (NE margin of Irian Jaya) and eastern Atlantic Ocean (Sierra Leone Rise), respectively. The five planktonic foraminifera species analyzed by *Bonneau et al.* [1980] showed a similar trend of calcite (104) XRD peak thinning with depth (Figure 1). In the present study, we decided to focus more particularly on the calcite crystallinity of the planktonic species *G. ruber*, a species particularly sensitive to dissolution [e.g., *Berger*, 1968, 1970], which makes it possible to address small-amplitude dissolution changes that may occur even above the lysocline.

[9] The comparison of Pacific and Atlantic Ocean depth transects is of particular interest for our purpose as the water column $CO_3^{=}$ profiles are largely different owing to the inter-basin, deep-water chemical contrast that results from the Great Conveyor Belt [*Broecker and Peng*, 1982]. These differences in the water column $CO_3^{=}$ profiles make it possible to test whether crystallinity changes are indeed strongly related to bottom water $CO_3^{=}$.

3. Material and Methods

[10] Surface sediments that we analyzed for this paper were sampled using a multicorer during 1998 winter cruise of the R/V *Knorr* (Sierra Leone Rise) and cruise IMAGES VII of the R/V *Marion Dufresne* in 2001 (Irian Jaya; Table 1). These data are compared to those obtained by *Bonneau et al.* [1980] on Ontong Java Plateau samples retrieved during cruise Eurydice of the R/V *Thomas Washington*, in 1975.

[11] Top sediment samples (upper centimeter) were wet-sieved on a 150 μm mesh-sieve and the coarse fraction dried overnight at 50°C. For the *G. ruber* XRD analyses, the samples were then dry-sieved and 80–100 shells were hand-picked in the 250–315 μm size fraction. *G. ruber* shells were soaked in methanol and ultrasonically cleaned in order to remove fines that could fill the last chambers. The purpose of such a cleaning procedure is to reduce the contribution of coccolith calcite to the XRD

Table 1. Locations of Samples Used for Crystallinity Studies

Site	Latitude	Longitude	Water Depth, m
Sierra Leone Rise (Eastern Equatorial Atlantic)			
Station A	5°07 N	21°00 W	2750
Station B	5°25 N	21°31 W	3200
Station C	5°32 N	21°48 W	3560
Station D	5°50 N	22°48 W	3890
Station E	7°00 N	24°37 W	4250
Station F	7°43 N	24°37 W	4750
Ontong Java Plateau (Western Equatorial Pacific)			
92 BX	2°13.5 S	156°59.9 E	1598
88 BX	0°02.9 S	155°52.1 E	1924
120 BX	0°01.0 S	158°41.6 E	2247
79 BX	2°47.1 N	156°13.8 E	2767
125 BX	0°00.2 S	160°59.9 E	3368
136 BX	1°06.0 N	161°36.3 E	3848
131 BX	0°01.6 S	162°41.1 E	4441
Irian Jaya Shelf Slope (Western Equatorial Pacific)			
MD122-MC05	0°48.31 S	134°28.79 E	1188
MD122-MC06	0°15.88 S	134°14.55 E	2110

crystallinity results. For the Sierra Leone Rise, mean shell weight of *G. ruber* picked from the same, narrow size fraction 250–315 μm was also measured in order to compare the crystallinity results with the normalized shell weight dissolution index [*Lohmann*, 1995].

[12] Because the broadening of foraminiferal calcite X-ray diffraction peak is likely related to the size of the perfectly crystallized subdomains that constitute the calcite, it is crucial that the sample preparation does not introduce a granulometry bias. Thus we did not prepare powders for X-ray diffraction through grinding in a mortar, but we followed the method from *Barthelemy-Bonneau* [1978] and we crushed very gently *G. ruber* shells with a glass slide, directly in the sample holder. Nonpublished, Coulter Counter grain size analyses performed on coarse-grained foraminifera powders prepared following this technique indicate that these powders have a mean grain size in the range 10–16 μm, with most of the grains larger than 4–5 μm (S. Birse, personal communication, Cambridge, 2004). This is too coarse a granulometry to introduce a bias in the width of calcite XRD peak since apparent grain size of crystallite affecting XRD peak broadening is smaller than a few tenth of micrometers. Thus our sample preparation technique insures that no peak-broadening bias is introduced and that data genuinely reflect calcite crystallinity from the foraminifera shells.

[13] Calcite crystallinity of samples from Sierra Leone Rise and Irian Jaya were analyzed at the Laboratoire de Géologie (MNHN, Paris) using the same XRD system and setups than *Bonneau et al.* [1980]. The system is a Siemens counting XRD device equipped with a thin Cu X-ray tube (optical width 40 μm) and a fast-rotating sample holder [*Mélières*, 1973]. Analytical setups for the XR beam were the following: entrance slot 0.5°, vertical collimator 2 mm, counting aperture 0.2 mm. The goniometer rotation speed was set to 0.25°2θ/mn.

[14] On a given X-ray diffractometer, even a perfect crystal lattice would show a certain degree of peak broadening, the so-called "instrumental width", which results from such factors as slit width, penetration in the sample, or imperfect focusing. In order to check whether our data could be directly compared to those obtained by *Bonneau et al.* [1980] or if a correction was necessary to account for the instrumental width, we reanalyzed a coarse-grained calcite powder (prepared from a well-crystallized Iceland Spar) that was analyzed at the time of Bonneau et al.'s work. The calcite (104) FWHM measurements we performed yields the same average value (0.125 ± 0.001°2θ) as that obtained during Bonneau et al.'s work (F. Mélières, unpublished data, 1979), indicating that our recent calcite (104) FWHM could be directly compared to those obtained by *Bonneau et al.* [1980].

[15] Each sample was run three times, then the powder was removed from the sample holder, mixed and reinserted in the sample holder to be run three additional times. Average value of calcite (104) FWHM and the related standard deviation were calculated from those six runs (except for Station B on Sierra Leone Rise where the data is an average of two replicate analyses performed on two distinct sets of ~80 shells picked from the Station B sample). The internal standard deviation varies from 0.001 to 0.004°2θ (1σ) with a mean value of about 0.002°2θ for XRD analyses that we performed on Sierra Leone Rise and Irian Jaya samples for this study. This variability is higher than that observed by *Bonneau et al.* [1980] in Ontong Java Plateau samples, which show an internal standard deviation of 0.001°2θ (1σ). It is not fully clear yet whether the higher internal standard deviation of our recent analyses is related to a higher heterogeneity of the Sierra Leone Rise and Irian Jaya *G. ruber* samples compared to Ontong Java Plateau samples, or if this points toward an increased instability of the X-ray diffractometer since its use by *Bonneau et al.* [1980]. In any case, the larger internal deviations shown by

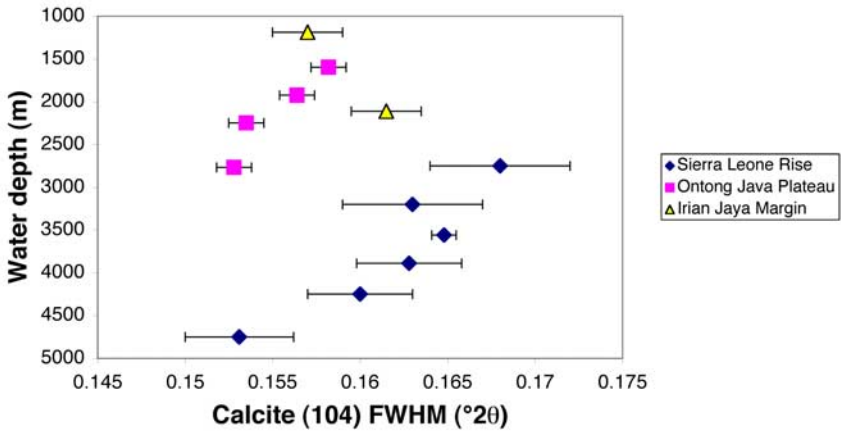

Figure 2. Profiles water depth versus calcite (104) FWHM of *Globigerinoides ruber* shells picked from surface samples along three depth transects: Ontong Java Plateau and Irian Jaya shelf slope (western equatorial Pacific); Sierra Leone Rise (tropical Atlantic Ocean). Data from Ontong Java Plateau are from *Bonneau et al.* [1980]. Standard deviations (1σ) were calculated from six consecutive measures of the calcite (104) peak width obtained from the same powder (see text for details).

XRD analyses on Sierra Leone Rise and Irian Jaya samples do not affect our interpretation since changes in calcite (104) FWHM along the depth transects studied are larger than internal standard deviation.

4. Results

4.1. Crystallinity Versus Depth Profiles

[16] In good accordance with the Ontong Java Plateau data from *Bonneau et al.* [1980], our data from Sierra Leone Rise show a general trend of thinning of calcite (104) peak (improving crystallinity) with increasing water depth (Figure 2 and Table 2). Station B departs noticeably from this general trend versus water depth, however. This may reflect local variability in sedimentation and/or early diagenesis processes (see below).

[17] Unlike Ontong Java Plateau and Sierra Leone Rise transects, the two data from the Irian Jaya transect show an opposite trend with water depth: at the deepest site MC06 (2210 m) the calcite (104) peak is broader (0.162°2θ) than at the shallower site MC05 (0.157°2θ at 1188 m). This value of 0.162°2θ at site MC06 appears to be high compared to values obtained by *Bonneau et al.* [1980] at about the same depth range on Ontong Java Plateau, the other western Pacific depth transect (Figure 2). This apparently anomalous value may

Table 2. Crystallinity Data[a]

Site	*G. ruber*	*S. dehiscens*	*G. tumida*	*P. obliquiloculata*
92 BX	0.158 ± 0.001	0.145 ± 0.001	0.147 ± 0.001	0.153 ± 0.001
88 BX	0.156 ± 0.001	0.143 ± 0.001	0.145 ± 0.001	0.149 ± 0.001
120 BX	0.153 ± 0.001	0.142 ± 0.001	0.143 ± 0.001	0.149 ± 0.001
79 BX	0.153 ± 0.001	0.140 ± 0.001	0.142 ± 0.001	0.147 ± 0.001
125 BX		0.140 ± 0.001	0.138 ± 0.001	0.145 ± 0.001
136 BX		0.135 ± 0.001	0.137 ± 0.001	0.142 ± 0.001
131 BX		0.131 ± 0.001	0.133 ± 0.001	0.138 ± 0.001
Station A	0.168 ± 0.004			
Station B	0.163 ± 0.004			
Station C	0.165 ± 0.001			
Station D	0.163 ± 0.003			
Station E	0.160 ± 0.003			
Station F	0.153 ± 0.003			
MD122-MC05	0.157 ± 0.002			
MD122-MC06	0.162 ± 0.002			

[a] Calcite (104) FWHM given in °2θ.

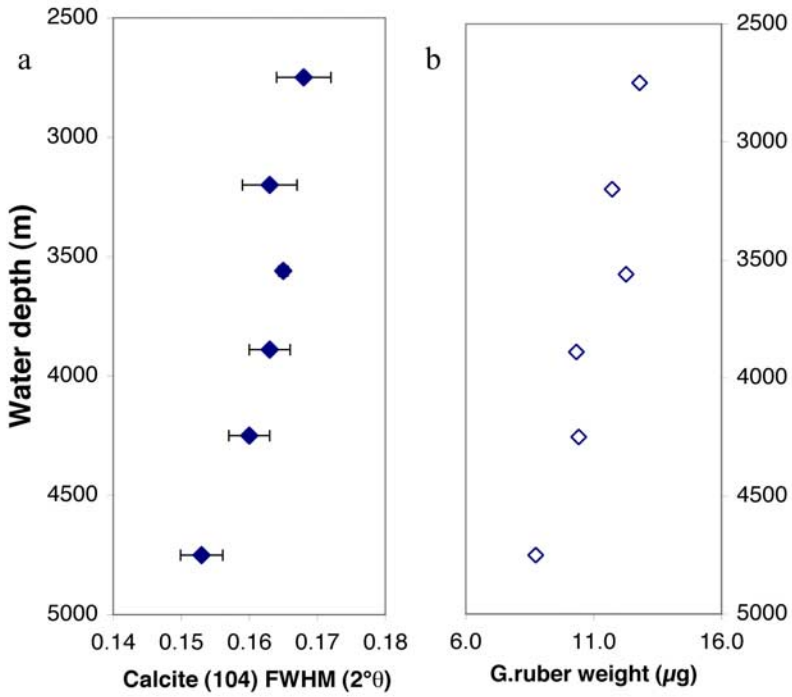

Figure 3. (a) Water depth versus calcite (104) FWHM for *Globigerinoides ruber* shells picked from surface samples along the Sierra Leone Rise transect, tropical Atlantic Ocean. Standard deviations (1σ) were calculated from six consecutive measures of the calcite (104) peak width from the same powder (see text for details). (b) Water depth versus *G. ruber* shell weight (size fraction 250–315 μm). Standard deviations (1σ) were calculated from measurements of ten subsamples of ~25 *G. ruber* shells each.

indicate that *G. ruber* shells picked at site MC06 have been brought recently to this water depth by down slope transport. Their crystallinity would be indicative of dissolution intensity at a shallower depth. Alternatively, this data may points toward important variability in local sedimentation processes (i.e., sedimentation rate, benthic activity). Additional data are necessary to solve that problem. For the time being, we decided to reject the MC06 data.

4.2. Crystallinity and Foraminifera Dissolution

[18] *Barthelemy-Bonneau* [1978] analyzed several dissolution indices in samples from the Ontong Java Plateau in order to check whether changes in the FWHM of calcite (104) XRD peak measured from foraminifera tests are related to dissolution. She showed, for instance, that the thinning of the (104) diffraction peak (improvement in foraminifera crystallinity) along the Ontong Java Plateau depth transect was accompanied by an increase in the overall fragmentation of the foraminifera assemblages. This increased fragmentation resulted in a concomitant change in granulometry, with a relative increase of the finest fraction due to the progressive transfer of fragments from the coarser fractions. Even more convincingly, *Barthelemy-Bonneau* [1978] displayed a set of SEM photographs, which showed that changes in crystallinity of the planktonic foraminifera tests were accompanied by dissolution-induced changes of their structure and texture.

[19] In order to confirm the link between foraminifera crystallinity and calcite dissolution on the Sierra Leone Rise transect, we compared the FWHM of calcite peak (104) with *G. ruber* shell weight dissolution index [e.g., *Lohmann*, 1995]. For this purpose, we measured the average shell weight of *G. ruber* in the same, narrow size fraction (250–315 μm) in which foraminifera tests were picked for XRD analyses. As can be seen in Figure 3, the general trend of peak (104) thinning with increasing water depth of deposition (Figure 3a, left) is consistent with an overall decrease in the average *G. ruber* shell weight (Figure 3b, right). Although the correlation between the two curves is very strong, they are not mimic image of each other, which may point toward a difference in the dissolution sensitivity of these two proxies and/or indicate that factors other than dissolution may affect their depth profiles. As stated

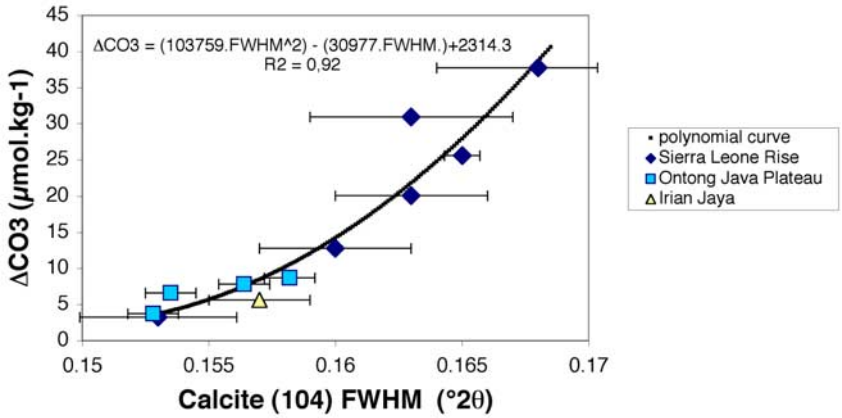

Figure 4. ΔCO_3 (=CO_3 − CO_{3crit}) versus calcite (104) FWHM of *G. ruber*. Data from Sierra Leone Rise, Irian Jaya, and Ontong Java Plateau depth transects are plotted with a second-order polynomial regression curve. Standard deviations (1σ) of data were calculated from six consecutive measures of the calcite (104) peak width from the same powder (see text for details). (Data from Ontong Java Plateau are from *Bonneau et al.* [1980].)

above, Station B is singled out in the Sierra Leone depth transect with both the *G. ruber* crystallinity and shell weight pointing toward an anomalously intense dissolution at this water depth.

[20] Our data and those from *Barthelemy-Bonneau* [1978] do indicate that changes in the FWHM of calcite peak (104) measured from planktonic foraminifera shells retrieved along depth transects are primarily related to dissolution at the seafloor. Assuming that the calcite (104) FWHM that we measured for the coarse-grained, well-crystallized Iceland Spar sample (0.125°2θ) is indicative of the diffractometer instrumental width, we can convert *G. ruber* peak broadening to average size of calcite crystallites using the Scherrer formula [*Warren*, 1969]:

$$D = K\lambda/B\cos\theta, \quad (1)$$

where D is the average crystallite size perpendicular to the reflection planes, λ is the X-ray wavelength, B is the peak broadening calculated as the peak FWHM minus the instrumental width (in radians), and θ is the diffraction angle of the diffraction peak (i.e., 0.257 radians for calcite (104) diffraction peak). K is a constant whose value depends on shape of crystallites. Theoretical values found in the literature vary from 0.89 to 1.07 [*Lipson and Steeple*, 1970]. In our calculations, we used K = 1 and refer therefore to an ''apparent'' crystallite size [*Lipson and Steeple*, 1970].

[21] When converted using the Scherrer formula, our XRD data show that along the Ontong Java Plateau transect, mean crystallite size of *G. ruber* varies from ~0.25 μm at 1598 m (sample 92BX) to 0.30 μm at 2767 m (sample 79BX), whereas along the Sierra Leone Rise transect, mean crystallite size varies from 0.19 μm at 2750 m (Station A) to 0.29 μm at 4750 m (station F). This increase of the mean, apparent crystallite size of *G. ruber* calcite along the depth transects indicates that dissolution proceeds by removing preferentially the shell parts that are made of calcite with the smallest crystallites.

4.3. Relationship Between Crystallinity of *G. ruber* and Bottom Water $\Delta CO_3^=$

[22] In order to test whether bottom water carbonate ion concentration is indeed a major factor in controlling foraminifera crystallinity through preferential dissolution at the bottom water-sediment interface, one needs to relate the measured calcite (104) FWHM and the departure of local bottom water from calcite saturation (ΔCO_3 = $CO_3^=$ − $CO_{3\ sat}^=$). We estimated bottom water $CO_3^=$ at our sites using *Archer* [1996] empirical equation applied to gridded T, S, O_2 and nutrients data [*Levitus*, 1994]. Then, the distance from calcite saturation (ΔCO_3) was calculated using a revised version of *Broecker and Takahashi* [1978] critical CO_3 equation (see Appendix A for details):

$$CO_{3\ crit}^= = 41.85\exp(0.173z), \quad (2)$$

where z is the water depth in kilometers.

[23] A good overall correlation is readily observed between the FWHM of *G. ruber* calcite (104) peak from the three transects, in the one hand, and bottom water ΔCO_3, in the other hand (Figure 4). Station B (Sierra Leone Rise transect) is, however,

noticeably off the other points. An empirical, second-order polynomial equation fit through the data gives a coefficient of correlation of $R^2 = 0.92$ (Figure 4). Taken at face value, this strong, empirical relationship between calcite (104) FWHM and bottom water ΔCO_3 indicates that crystallinity of *G. ruber* from core top samples could be a promising proxy for the carbonate ion content in modern tropical ocean deep water.

[24] This raises questions about the nature (thermodynamic equilibrium versus kinetic control) of the relationship between crystallinity and bottom water carbonate ion content. The covariation between bottom water $CO_3^{=}$ and crystallinity could reflect changes in calcite solubility. Would it be the case, calcite crystallinity would provide a direct proxy of bottom water $CO_3^{=}$. However, independent evidence from equilibration experiments (M. Gehlen et al., Reassessing the dissolution of marine carbonates: I. Solubility, submitted to *Deep Sea Research*, 2004) using foraminifer assemblages sampled along the Ontong Java Plateau and Sierra Leone Rise transects is not in favor of this hypothesis. Experimental concentration products $[CO_3^{2-}] \times [Ca^{2+}]$ correspond to the stoichiometric solubility product (Ksp) of synthetic calcite [*Mucci*, 1983], and they do not evolve with depth as dissolution proceeds. Thus changes in foraminiferal crystallinity likely reflect a kinetic effect, with the preferential dissolution of shell parts with the smallest calcite crystallites. In that case, planktonic shell crystallinity is an indirect proxy of bottom water $CO_3^{=}$, much in the same way as shell weight [*Broecker and Clark*, 2001a, 2001b] or $CaCO_3$ size distribution [*Broecker and Clark*, 1999].

4.4. Extending the Foraminifera Crystallinity Proxy to Lower Bottom Water $CO_3^{=}$

[25] As mentioned above, our initial interest for testing *G. ruber* crystallinity as a dissolution proxy was motivated by the fact that *G. ruber* is one of the most dissolution-sensitive planktonic foraminifera species [e.g., *Berger*, 1968, 1970]. This limits, however, the use of *G. ruber* crystallinity as a carbonate ion proxy to shallow, supra-lysoclinal water masses. Indeed, the proportion of *G. ruber* within the foraminifera assemblages drops rapidly near the lysocline. This explains why *Bonneau et al.* [1980] could not find enough whole *G. ruber* shells to perform crystallinity analyses at depths greater than ~2800 meters along the Ontong Java Plateau transect (about 600 m above the local lysocline). Similarly, we were not able to extract enough whole *G. ruber* tests at the deepest of the Sierra Leone Rise sites (station G at 4950 m of water depth). In order to reconstruct $CO_3^{=}$ changes in bottom waters at or below the lysocline, solution-resistant planktonic foraminifera shells are needed.

[26] *Bonneau et al.* [1980] analyzed dissolution-resistant species such as *S. dehiscens*, *P. obliquiloculata* and *G. tumida*. They might be good candidates for developing a crystallinity-based CO_3 proxy at or below the calcite lysocline. These species were successfully picked at water depths down to 4440 meters on Ontong Java Plateau (corresponding to bottom water ΔCO_3 of about -9 $\mu mol.kg^{-1}$; Figure 5). Within the range of ΔCO_3 variability along the Ontong Java Plateau transect, the specific relationships between calcite (104) FWHM width and ΔCO_3 are best approximated by simple linear regressions for the dissolution-resistant species (Figure 5). As can be readily seen from Figure 5, the rates (slopes) of change of calcite (104) FWHM with decreasing ΔCO_3 are remarkably similar from one foraminifera species to the other, which indicates that relative changes in mean crystallite size of foraminiferal calcite induced by increasing dissolution are remarkably coherent for the four species studied.

5. Discussion

[27] Our data showed that calcite (104) FWHM of foraminifera shell calcite is related to dissolution intensity and could be used to estimate bottom water carbonate ion concentration in today's tropical bottom waters. The strong relationship between the calcite (104) FWHM and bottom water ΔCO_3 indicates that most of the crystallinity variance is linked to changes in bottom water ΔCO_3. The departure of station B (Sierra Leone Rise) *G. ruber* crystallinity from the other data reminds us, however, that local processes may alter noticeably the relationship between dissolution intensity in surface sediments and bottom water $CO_3^{=}$.

[28] We know that supra-lysoclinal dissolution requires metabolic CO_2 to be produced through oxic degradation of organic matter [*Emerson and Bender*, 1981]. This in situ production of CO_2 drives pore water $CO_3^{=}$ away from the initial bottom water carbonate ion concentration, explaining how undersaturation might be reached and dissolution occurs within supra-lysoclinal sediments. Given the need of respiration CO_2 to drive supra-lysoclinal dissolution, the overall, striking coherency of the "*G. ruber* crystallinity versus bottom water ΔCO_3"

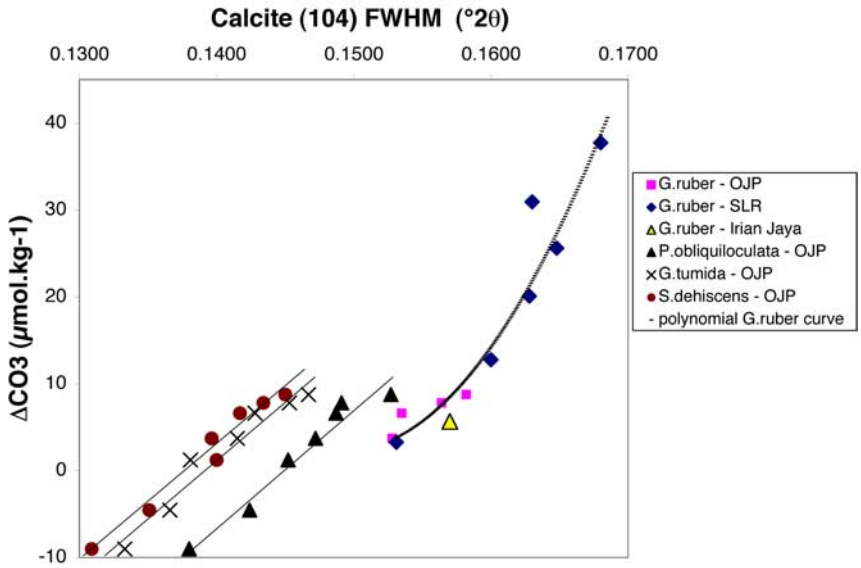

Figure 5. ΔCO_3 (=CO_3 − CO_{3crit}) versus calcite (104) FWHM of four planktonic species (*G. ruber*, *P. obliquiloculata*, *G. tumida*, and *S. dehiscens*). *G. ruber* data are displayed with the second-order polynomial regression curve shown in Figure 4, and the three other species are plotted with linear regression fits: *S. dehiscens*, ΔCO_3 = 1345.2FWHM − 185.44 (R^2 = 0.97); *G. tumida*, ΔCO_3 = 1343.4FWHM − 186.84 (R^2 = 0.95); *P. obliquiloculata*, ΔCO_3 = 1351.7 − 195.53 (R^2 = 0.96). (Data from Ontong Java Plateau are from *Bonneau et al.* [1980].) OJP, Ontong Java Plateau; SRL, Sierra Leone Rise.

relationship at three different geographic locations (Figure 4) may appear puzzling. The production of metabolic CO_2 and the related supra-lysoclinal carbonate dissolution is a complex mechanism that depends on many parameters such as organic carbon rain, sediment composition, mixing rate, or bottom water oxygenation. Among these parameters, the Corg/$CaCO_3$ ratio of the flux reaching the seafloor plays a key role [*Emerson and Bender*, 1981]. *Klaas and Archer* [2002], using sediment trap data, showed that most of organic carbon rain to the deep sea (∼83%) is carried by calcium carbonate owing to its overall abundance in the pelagic rain and its efficiency as a ballast mineral [*Armstrong et al.*, 2002; *François et al.*, 2002]. Below the first kilometer in the water column (over which the more labile, "free" particulate organic carbon (POC) is rapidly oxidized), sediment trap data show little variability of organic carbon to calcium carbonate rain ratios to the deep sea. The Corg/$CaCO_3$ ratio averages 0.768 ± 0.197 for sites deeper than 2000 m, and 0.719 ± 0.215 for sites deeper than 3000 m. We suggest that the worldwide near constancy in the deep-sea Corg/$CaCO_3$ rain ratio may be an important factor in setting the relationship between supra-lysoclinal *G. ruber* crystallinity and bottom water ΔCO_3 and could play a role in the overall good coherency between our three remote depth transects.

[29] The efficiency of pelagic carbonate as a ballast mineral and the resulting strong covariance between Corg and $CaCO_3$ in the pelagic rain imply that the mean Corg/$CaCO_3$ ratio reaching the deep sea had probably undergone only little changes through time. As pointed out by *Ridgwell* [2003], such a buffering of Corg/$CaCO_3$ flux ratios introduces a major drawback for the rain ratio hypothesis, which seeks to explain a large part of glacial-interglacial atmospheric CO_2 changes [*Archer and Maier-Reimer*, 1994]. In terms of developing a bottom water $CO_3^{=}$ index based on dissolution proxies such as foraminifera crystallinity, however, such a Corg/$CaCO_3$ buffering has an interesting implication: the empirical relationships obtained between foraminifera crystallinity and bottom water ΔCO_3 in our modern calibration exercise should remain largely valid under past conditions.

6. Conclusion

[30] Our data confirm and extend the qualitative work of *Bonneau et al.* [1980] by demonstrating that calcite (104) FWMH of foraminifera shells (an index of their crystallinity) could be used as a proxy to estimate bottom water carbonate ion concentration in tropical bottom waters. Except from specific areas where surface productivity

and sedimentation have undergone major changes in the past, the rather constant Corg/$CaCO_3$ rain ratio in the deep ocean [*Klaas and Archer*, 2002] and its likely buffering in the past [*Ridgwell*, 2003] may indicate that today's empirical relationship between *G. ruber* crystallinity (or crystallinity from other planktonic species) and bottom water $CO_3^=$ should remain valid for estimating past carbonate ion content of bottom water.

Appendix A: Calculation of Saturation Relative to Calcite: A Revised $CO_3^={}_{crit.}$ Equation

A1. Bottom Water $CO_3^=$: *Archer*'s [1996] Gridded Estimates

[31] As there are no hydrographic database that provides $CO_3^=$ measurements in the close vicinity of all our Atlantic and Pacific sites, we used the empirical, multiparameter equation developed by *Archer* [1996] to estimate $CO_3^=$ profiles from Levitus hydrographic gridded T, S, O_2 and nutrient database [*Levitus*, 1994]. For each of the three depth transect areas, we developed a mean $CO_3^=$ profile, averaged from several $CO_3^=$ profiles computed at the Levitus sites nearest to our core top locations. This $CO_3^=$ averaging procedure leads to RMS deviations ranging from 0.5 to 3.5 $\mu mol.kg^{-1}$. The final step of estimating $CO_3^=$ at our core top locations consisted in interpolating the $CO_3^=$ data, estimated at the Levitus depth levels, to the water depths of our samples. At the end, the error bar associated to $CO_3^=$ estimates is in the range of ± 10 $\mu mol.kg^{1}$. This is a large error bar considering that the differences in bottom water $CO_3^=$ along our three depth transects range from 7 $\mu mol.kg^{-1}$ (Sierra Leone Rise) to 13 $\mu mol.kg^{-1}$ (Ontong Java Plateau). Hopefully, most of this error bar reflects random variability (i.e., analytical noises imbedded in the original hydrographic database) and should not result in systematic biases when comparing our three depth transects.

A2. Estimating Calcite Saturation: A Revised Critical $CO_3^=$ Equation

[32] Once we have determined the carbonate ion of the bottom water at our sites, one still has to estimate the "distance from calcite saturation", since dissolution of calcite is driven by the difference between the actual water $CO_3^=$ and the $CO_3^=$ at saturation [e.g., *Keir*, 1980]. However, the calculation of saturation relative to calcite at depth in the water column is not trivial. The pressure dependency of the calcite solubility product (Ksp) is still under debate. Ultimately, this pressure dependency rests upon the volume difference (ΔV) between calcite and its ionic dissolution products [*Millero*, 1979]. Using the smallest ($\Delta V = -36$ $cm^3.mole^{-1}$ [*Culberson*, 1972]) or the highest ($\Delta V = -44$ $cm^3.mole^{-1}$ [*Ingle*, 1975; *Sayles*, 1980]) of the volume change estimates found in the literature results in differences of up to 6% per kilometer in the normalization of $CO_3^=$ profiles when correcting Ksp for pressure using the equation given by *Millero* [1979]. In order to avoid making initial assumptions about the solubility of calcite within the water column and/or the pressure dependence of Ksp we decided to follow *Broecker and Takahashi* [1978] to calculate the shift from calcite saturation at depth. These authors developed an empirical equation of "critical $CO_3^=$" versus water depth by fitting a regression equation through a set of lysocline $CO_3^=$ values, and using departure from equilibrium $CO_3^=$ computed from several water column saturometry measurements [e.g., *Ben Yaakov et al.*, 1974]. Using directly *Broecker and Takahashi*'s [1978] $CO_3^={}_{crit}$ equation, however, would not insure an adequate internal consistency with our own $CO_3^=$ database. Indeed, the *Archer* [1996] empirical equation that we use to calculate $CO_3^=$ profiles has been computed from the GEOSECS $CO_3^=$ database, but this database has been corrected since its use by Broecker and Takahashi in 1978. Corrections were applied to TCO_2 and Alkalinity data to improve the consistency of the GEOSECS database with the more recent TTO/NAS data. The rationale of these corrections is given by *Takahashi* [1982, pp. 5 and 6], *Takahashi* [1983, pp. 6 and 7], and *Takahashi et al.* [1985]. Thus, in order to be fully consistent with our estimated $CO_3^=$ profiles, we decided to compute a revised critical $CO_3^=$ equation using the same lysocline and saturometry data that were used by *Broecker and Takahashi* [1978], but based on $CO_3^=$ profiles computed from the corrected GEOSECS database. The resulting critical $CO_3^=$ equation is

$$CO_{3\,crit}^= = 41.85 \exp(0.173z), \quad (2)$$

where z is the water depth in kilometers.

[33] It should be noted that our strategy differs slightly from that of Broecker and Takahashi as we forced the $CO_3^={}_{crit.}$ at the sea surface to 41.85 $\mu mol.kg^{-1}$, based on the Ksp value computed from *Mucci*'s [1983] equation with S = 35‰ and T = 3°C (these salinity and temperature

values correspond to the average hydrographic conditions at the depth of lysocline and saturometry data). The purpose of forcing $CO_3^{=}$ at the sea surface in our revision of Broecker and Takahashi's equation is to solve an ambiguity carried on by the in situ saturometry data. *Broecker and Takahashi* [1978] used in situ saturometry data from three deployments, two of them around Hawaii [*Ben Yaakov et al.*, 1974]. Empirical $CO_{3\ crit}^{=}$ regression equations computed using either the Northern or the Southern of these two Hawaiian sets of saturometry data differ both in their intercept value at sea surface and their slope. The Northern data yields and intercept at sea surface (41.2 $\mu mol.kg^{-1}$) which is remarkably close to $CO_3^{=}$ that was independently computed from *Mucci*'s [1983] equation of Ksp for surface seawater: 41.85 $\mu mol.kg^{-1}$. Using the Southern saturometry data set, however, leads to a quite different $CO_3^{=}$ intercept at the sea surface (50.4 $\mu mol.kg^{-1}$). We do not have an explanation for this difference between the two saturometry data sets, nor can we confidently eliminate those data that could be erroneous. However, as it appears unlikely that the good match with the independent $CO_3^{=}$ estimate at sea surface obtained from Mucci's equation could be completely fortuitous, we decided to force the equation to intercept at 41.85 $\mu mol.kg^{-1}$ at the sea surface.

Acknowledgments

[34] M.G. acknowledges the hospitality received during the cruise KN159. Special thanks to the crew of R/V *Knorr* and all the cruise participants for their help and support. F.B. thanks the crew of the R/V *Marion Dufresne* and the team from IPEV (Brest) for their help and support during IMAGES VII - WEPAMA cruise. We thank T. Takahashi, H. Elderfield, S. Weiner, S. Birse, D. McCorkle, J. Erez, and D. Archer for invaluable discussions. A review by B. Hales, P. Dovee, and M. Delaney improved the paper. This work was made possible through financial support by French INSU/CNRS-ECLIPSE program, European contract CESOP EVR1-2001-40018, as well as basic support from CEA and CNRS to the LSCE. This is IPSL contribution LSCE 1201.

References

Anderson, D. M., and D. Archer (2002), Glacial-interglacial stability of ocean pH inferred from foraminifer dissolution rates, *Nature*, *416*, 70–73.

Archer, D. E. (1996), An atlas of the distribution of calcium carbonate in sediments of the deep sea, *Global. Biogeochem. Cycles*, *10*, 159–174.

Archer, D., and E. Maier-Reimer (1994), Effect of deep-sea sedimentary calcite preservation on atmospheric CO_2 concentration, *Nature*, *367*, 260–263.

Armstrong, R. A., C. Lee, J. I. Hedges, S. Honjo, and S. G. Wakeham (2002), A new, mechanistic model for organic carbon fluxes in the ocean based on the quantitative association of POC with ballast minerals, *Deep Sea Res., Part II*, *49*, 219–236.

Barker, S., and H. Elderfield (2002), Foraminiferal calcification response to glacial-interglacial changes in atmospheric CO_2, *Science*, *297*, 833–836.

Barthelemy-Bonneau, M.-C. (1978), Dissolution expérimentale et naturelle de foraminifères planctoniques—Approches morphologique, isotopique et crystallographique, Ph.D. thesis, 231 pp., Univ. Pierre et Marie Curie, Paris.

Ben Yaakov, S., E. Ruth, and I. R. Kaplan (1974), Carbonate compensation depth: Relation to carbonate solubility in ocean waters, *Science*, *184*, 982–984.

Berger, W. H. (1968), Planktonic foraminifera: Selective solution and paleoclimatic interpretation, *Deep Sea Res. Oceanogr. Abstr.*, *15*, 31–43.

Berger, W. H. (1970), Planktonic foraminifera: Selective solution and the lysocline, *Mar. Geol.*, *8*, 111–138.

Bijma, J., B. Hönisch, and R. E. Zeebe (2002), Impact of the ocean carbonate chemistry on living foraminiferal shell weight: Comment on "Carbonate ion concentration in glacial-age deep waters of the Caribbean Sea" by W. S. Broecker and E. Clark, *Geochem. Geophys. Geosyst.*, *3*(11), 1064, doi:10.1029/2002GC000388.

Bonneau, M. C., F. Mélières, and C. Vergnaud-Grazzini (1980), Variations isotopiques (oxygène et carbone) et crystallographiques chez des espèces actuelles de foraminifères planctoniques en fonction de la profondeur de dépôt, *Bull. Soc. Geol. Fr.*, *22*(5), 791–793.

Boyle, E. A. (1988), Vertical oceanic nutrient fractionation and glacial/interglacial CO_2 cycles, *Nature*, *331*, 55–56.

Broecker, W. S., and E. Clark (1999), $CaCO_3$ size distribution: A paleocarbonate ion proxy?, *Paleoceanography*, *14*(5), 596–604.

Broecker, W. S., and E. Clark (2001a), Glacial-to-Holocene redistribution of carbonate ion in the deep sea, *Science*, *294*, 2152–2155.

Broecker, W. S., and E. Clark (2001b), An evaluation of Lohmann's foraminifera weight dissolution index, *Paleoceanography*, *16*, 531–534.

Broecker, W. S., and T. H. Peng (1982), *Tracers in the Sea*, Lamont-Doherty Earth Obs., 690 pp., Palisades, N. Y.

Broecker, W. S., and T. H. Peng (1987), The role of $CaCO_3$ compensation in the glacial to interglacial atmospheric CO_2 change, *Global Biogeochem. Cycles*, *1*(1), 15–29.

Broecker, W. S., and T. H. Peng (1989), The cause of the glacial to interglacial atmospheric CO_2 change: A polar alkalinity hypothesis, *Global Biogeochem. Cycles*, *3*(3), 215–239.

Broecker, W. S., and T. Takahashi (1978), The relationship between lysocline depth and in situ carbonate ion concentration, *Deep Sea Res.*, *25*, 65–95.

Culberson, C. H. (1972), Processes affecting the oceanic distribution of carbon dioxide, Ph.D. thesis, 178 pp., Oregon State Univ., Corvallis.

Emerson, S., and M. Bender (1981), Carbon fluxes at the sediment-water interface of the deep sea: Calcium carbonate preservation, *J. Mar. Res.*, *39*, 139–162.

François, R., S. Honjo, R. Krishfield, and S. Manganini (2002), Factors controlling the flux of organic carbon to the bathypelagic zone of the ocean, *Global Biogeochem. Cycles*, *16*(4), 1087, doi:10.1029/2001GB001722.

Ingle, S. E. (1975), The solubility of calcite in the oceans, *Mar. Chem.*, *3*, 301–319.

Keir, R. S. (1980), The dissolution kinetics of biogenic calcium carbonates in seawater, *Geochim. Cosmochim. Acta*, *44*, 241–252.

Klaas, C., and D. E. Archer (2002), Association of sinking organic matter with various types of mineral ballast in the deep sea: Implications for the rain ratio, *Global Biogeochem. Cycles*, *16*(4), 1116, doi:10.1029/2001GB001765.

Levitus, S. (1994), *Climatological Atlas of the World Ocean*, *NOAA Prof. Pap. 13*, Natl. Oceanic and Atmos. Admin, Silver Spring, Md.

Lipson, H., and H. Steeple (1970), *Interpretation of X-Ray Powder Diffraction Patterns*, 335 pp., MacMillan, Old Tappan, N. J.

Lohmann, G. P. (1995), A model for variation in the chemistry of planktonic foraminifera due to secondary calcification and selective dissolution, *Paleoceanography*, *10*, 445–457.

Mélières, F. (1973), Porte-échantillon tournant pour analyse par diffractométrie X, *Bull. Soc. Fr. Mineral. Cristallogr.*, *96*, 75–79.

Mélières, F. (1978), X-ray mineralogy studies, Leg 41, Deep Sea Drilling Project, Eastern North Atlantic Ocean, *Initial Rep. Deep Sea Drill. Proj.*, *41*, 1065–1086.

Millero, F. J. (1979), The thermodynamics of the carbonate system in seawater, *Geochim. Cosmochim. Acta*, *43*, 1651–1661.

Mucci, A. (1983), The solubility of calcite and aragonite in seawater at various salinities, temperatures and one atmosphere total pressure, *Am. J. Sci.*, *283*, 780–799.

Ridgwell, A. J. (2003), An end to the "rain ratio" reign?, *Geochem. Geophys. Geosyst.*, *4*(6), 1051, doi:10.1029/2003GC000512.

Sanyal, A., N. G. Hemming, G. N. Hanson, and W. S. Broecker (1995), Evidence for a higher pH in the glacial ocean from boron isotopes in foraminifera, *Nature*, *373*, 234–236.

Sayles, F. L. (1980), The solubility of $CaCO_3$ in seawater at 2°C based upon in-situ sampled pore water composition, *Mar. Chem.*, *9*, 223–235.

Takahashi, T. (1982), Precision of GEOSECS shipboard data, in *GEOSECS Pacific Expedition*, vol. 3, *Hydrographic Data*, edited by W. S. Broecker, D. W. Spencer, and H. Craig, pp. 5–10, Natl. Sci. Found., Washington, D. C.

Takahashi, T. (1983), Precision and accuracy of the GEOSECS Indian Ocean alkalinity and total CO_2 concentration data, in *GEOSECS Indian Ocean Expedition*, vol. 5, *Hydrographic Data, 1977–1978*, edited by R. F. Weiss et al., pp. 5–7, U.S. Govt. Print. Off., Washington, D. C.

Takahashi, T., W. S. Broecker, and S. Langer (1985), Redfield ratio based on chemical data from isopycnal surfaces, *J. Geophys. Res.*, *90*, 6907–6924.

Warren, B. E. (1969), *Diffraction by Imperfect Crystals in X-Ray Diffraction*, 251 pp., Dover, Mineola, N. Y.